communications biology

A Nature Portfolio journal

Article

https://doi.org/10.1038/s42003-026-11323-4

Shared and distinct neural pathways of aversive and appetitive pain-related learning

Check for updates

Jialin Li [1,2,4], Lea Busch [1,4], Katarina Forkmann[1], Tamas Spisak [1], Jaspreet Kaur[1], Frederik Schlitt-Nguyen [1], Katja Wiech [1,3], Katharina Schmidt [1,4] ✉ & Ulrike Bingel [1,4]

Aversive and appetitive learning are central to adaptive behaviour, and pain and avoidance are powerful examples of such forces shaping human behaviour. Alterations in learning are thought to contribute to the development and maintenance of chronic pain, yet their neural underpinnings remain unclear. In this registered within-subject fMRI study (German Clinical Trials Register, DRKS-ID: DRKS00027448), we examined both aversive and appetitive pain learning during acquisition and extinction in 68 healthy individuals. Ratings confirm successful learning, with exploratory analyses suggesting stronger aversive acquisition and incomplete extinction. Both conditions engage the visual cortex during acquisition, with increased connectivity to the right operculum. Aversive acquisition further elicits stronger mediodorsal thalamus activity and heightened connectivity with the locus coeruleus, alongside sustained parahippocampal activation during extinction. Incomplete aversive extinction is linked to ongoing visual cortex activity during pain anticipation. Findings suggest shared neural substrates, but stronger aversive recruitment of rapid encoding and persistent memory systems.

Human behaviour is guided by two key principles: avoiding harm and seeking conditions that ensure survival. Learning from cues that signal potential harm is therefore as crucial as learning from cues that predict desirable outcomes. Because of its inherently aversive nature, pain naturally captures attention and promotes avoidance learning[1,2]. Conversely, the alleviation of pain can be regarded as a rewarding experience, governed by the principles of appetitive learning[3]. When the cue is no longer followed by pain or relief, the CS-US associations (i.e., CS, conditioned stimuli; US, unconditioned stimuli) must be updated to allow for the meaningful prediction of future events[4] including the response to analgesic treatments. Impairments in acquiring and extinguishing cue–pain associations are thought to underlie not only chronic pain but also other conditions often comorbid with pain such as anxiety disorders, with direct implications for treatment efficacy[3,5,6].

Despite their complementary roles in adaptive behaviour, aversive and appetitive learning have often been studied in isolation, or across different modalities[7–13]. However, direct within-subject comparisons are essential to determine whether these two forms of learning rely on shared or distinct neural systems. Pain provides a particularly powerful model for such investigations because it naturally encompasses both aversive and appetitive learning within the same sensory modality. Whereas many studies compare learning across different stimulus domains (e.g., monetary reward versus threat), pain and pain relief arise from the same underlying sensory experience, allowing direct comparison of opposing motivational processes while minimising modality-specific confounds. An important exception is the study by Seymour and colleagues[14], which directly compared appetitive and aversive pain-related learning and demonstrated both shared and distinct neural prediction-error signals during ongoing probabilistic learning.

In a recent behavioural study using an established capsaicin-induced tonic heat pain model in healthy individuals, we paired predictive cues with either pain exacerbation or relief. This approach enabled simultaneous investigation of aversive and appetitive pain-related learning within the same sample. Results showed stronger acquisition during aversive (pain exacerbation) learning and incomplete extinction for aversive events[15], in line with previous results on comparing aversive and appetitive learning[16]. These findings are consistent with more recent evidence from placebo and nocebo research demonstrating that nocebo effects can be elicited by verbal

[1]Department of Neurology, Center for Translational Neuro- and Behavioral Sciences (C-TNBS), University Medicine Essen, University Duisburg-Essen, Essen, Germany. [2]Max Planck School of Cognition, Leipzig, Germany. [3]Wellcome Centre for Integrative Neuroimaging (WIN), Nuffield Department of Clinical Neurosciences, University of Oxford, John Radcliffe Hospital, Oxford, UK. [4]These authors contributed equally: Jialin Li, Lea Busch, Katharina Schmidt, Ulrike Bingel. ✉e-mail: katharina.schmidt@uk-essen.de

suggestion alone[17], are acquired more readily and persist longer than placebo effects[18], supporting the hypothesis that learning about potentially harmful events is prioritized over learning about beneficial ones. However, while these studies established a robust behavioural asymmetry, the neural mechanisms underlying these differences remained unclear. Here, we use the same capsaicin model as in our previous study to characterise how neural responses evoked by cues predicting pain exacerbation or pain relief change over the course of acquisition and extinction, and thereby investigate neural processes associated with the previously observed behavioural asymmetry between aversive and appetitive pain-related learning. Examining these changes across learning allows us to determine whether this behavioural asymmetry is paralleled not only by differences in the neural systems engaged, but also by differences in how their engagement develops during acquisition and persists during extinction. Thermal stimulation was applied to a capsaicin-pretreated area on the forearm in combination with individually calibrated temperatures to maintain moderate tonic pain throughout the experiment, with pain increase and pain decrease to induce pain exacerbation and relief, respectively. Geometrical cues ($CS_{increase}$, $CS_{decrease}$, CS_{medium}) signalled pain exacerbation ($US_{increase}$), pain relief ($US_{decrease}$), or no change in temperature (US_{medium}) during acquisition, while all cues were followed by unchanged stimulation (US_{medium}) during extinction (Fig. 1). CS-US learning was assessed through valence ratings to evaluate the affective dimension and contingency ratings to measure conscious learning. Participants also provided US pain intensity and (un) pleasantness ratings. Brain activity was recorded using functional magnetic resonance imaging (fMRI) during both the acquisition and extinction phase. Building on previous behavioural and neuroimaging findings, the present study extends the literature in three important ways. First, it characterises the neural responses to cues signalling pain exacerbation and pain relief and how these responses change over the course of acquisition and extinction within the same participants. Second, it directly compares shared and distinct neural systems supporting aversive and appetitive pain-related learning across both learning phases. Third, it relates these neural processes to the behavioural asymmetry previously observed in this paradigm, namely stronger acquisition and incomplete extinction of aversive pain learning. We hypothesised that (1) CS-US-associations related to pain exacerbation would be acquired more rapidly and extinguish more slowly than those for appetitive events and (2) aversive and appetitive learning would engage both shared and distinct neural networks across acquisition and extinction.

Our results show that pain exacerbation and pain relief learning engage partly shared neural systems during acquisition and extinction. Aversive learning is behaviourally stronger, extinguishes less completely, and preferentially recruits mediodorsal thalamic, locus coeruleus, parahippocampal, and occipital circuits linked to rapid encoding and persistent threat-related processing.

Results

Overview

A total of $n = 84$ healthy individuals were enrolled in the study to participate in a differential conditioning task during functional magnetic resonance imaging (fMRI) to compare aversive and appetitive acquisition and extinction learning using an experimental pain model. Data from $n = 16$ participants were excluded from the behavioural analyses for several reasons: the thermal stimuli ($US_{increase}$, $US_{decrease}$ and US_{medium}) could not be calibrated as intended or changed substantially during acquisition training (e.g., participants rated the US_{medium} as more painful than the $US_{increase}$, $n = 9$), early termination of the experiment by the participants ($n = 3$) and technical errors ($n = 4$). Following participant exclusion, behavioural results are based on $n = 68$ healthy participants ($n_{male} = 33$, $n_{female} = 35$, mean age = 37.65 ± 13.19 years), while fMRI results are based on $n = 61$ participants ($n_{male} = 31$, $n_{female} = 30$, mean age = 37.51 ± 13.28 years); $n = 7$ participants were excluded from the fMRI analysis due to missing data in either the brain structural or functional brain MRI images ($n = 6$) and the logfile ($n = 1$). Sample characteristics are shown in Supplementary Table S1.

In a within-subject design, participants learned to associate visual cues with an aversive increase ($CS_{increase}$), an appetitive decrease ($CS_{decrease}$), or no change (CS_{medium}) in noxious thermal input during acquisition training. In the subsequent extinction training, none of the cues was followed by changes in noxious input (see Methods for details on the paradigm). Behavioural measures of learning included CS valence ratings and CS-US

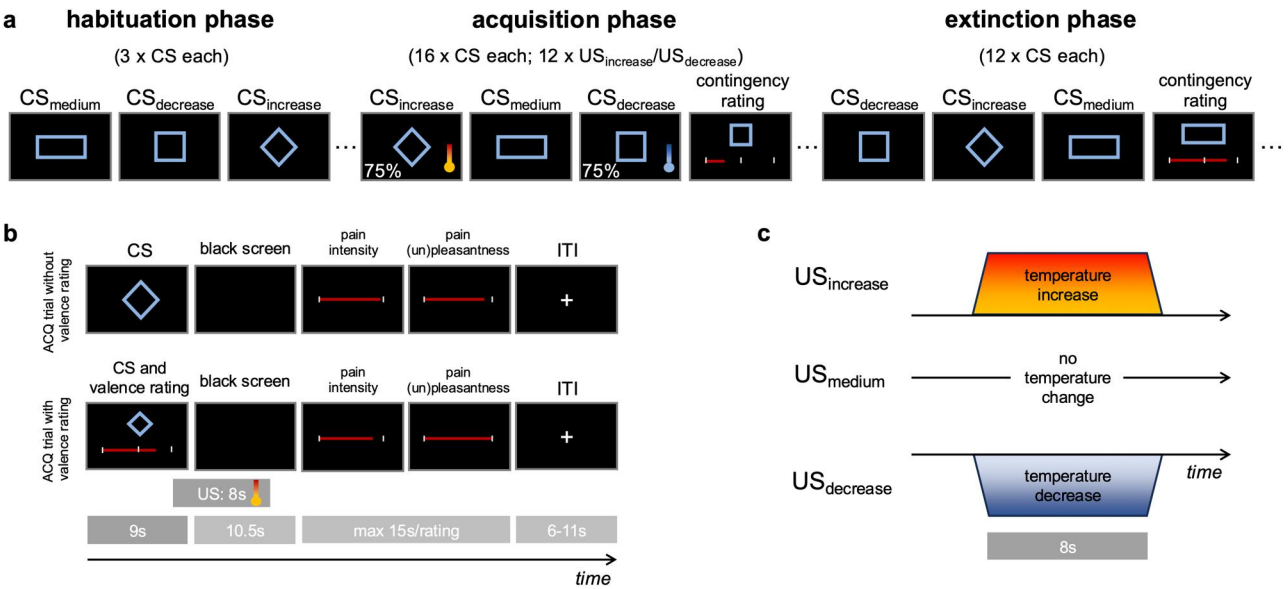


Fig. 1 | Study and trial design. a Study design with habituation, acquisition and extinction phase. During the acquisition phase, 75% of $CS_{increase}$ and $CS_{decrease}$ trials were followed by a temperature increase or temperature decrease, respectively. In the habituation and extinction phases, none of the CSs was reinforced. Contingency ratings were provided at the end of the acquisition and extinction phase for each CS separately. **b** Design of trials without (upper row) and with valence ratings (lower row) including pain intensity and (un)pleasantness ratings. **c** Temperature manipulation. The temperature of the thermal device was increased in the aversive (i.e., pain exacerbation) condition ($US_{increase}$, VAS80), decreased in the appetitive (i.e., pain relief) condition ($US_{decrease}$, VAS0) and kept constant in the control condition (US_{medium}, VAS40). CS conditioned stimulus, US unconditioned stimulus, ITI inter-trial interval.

contingency ratings and we identified joint and distinct changes in blood oxygenation level-dependent (BOLD) signals and functional connectivity of regions-of-interests (ROIs) across aversive and appetitive learning. To control for spontaneously occurring changes in outcome measures unrelated to temperature manipulations, all analyses compared behavioural and neural responses in the aversive and appetitive conditions against the control condition (i.e., $CS_{increase}$/$CS_{decrease}$ vs. CS_{medium}).

US pain intensity and (un)pleasantness ratings

Analyses of pain intensity and (un)pleasantness ratings obtained during acquisition training confirmed successful calibration of the noxious stimuli. Compared to the control condition, the thermal stimulation in the aversive condition was on average perceived as significantly more painful ($US_{increase} > US_{medium}$, $p < 0.001$; Table 1; Fig. 2a) and unpleasant ($US_{increase} > US_{medium}$, $p < 0.001$) and the stimulation in the appetitive condition as less painful ($US_{decrease} < US_{medium}$, $p < 0.001$; Table 1; Fig. 2a) and less unpleasant ($US_{decrease} < US_{medium}$, $p < 0.001$). Importantly, (un)pleasantness ratings for the US_{medium} did not significantly differ from zero ($t(67) = -0.90$, $p = 0.371$) during extinction training, indicating that the reference condition did not shift towards an appetitive state. For details, see Supplementary Results US pain intensity and US (un)pleasantness.

Behavioural evidence for acquisition and extinction learning

Our primary behavioural analyses addressed the main research question of differential aversive and appetitive learning on the emotional and cognitive level (i.e., valence and contingency ratings). Subsequent follow-up behavioural analyses including direct comparisons of CS-specific learning slopes, initial learning effects, and incomplete extinction were considered exploratory.

Acquisition

Valence ratings. Participants rated CS valence in every fourth trial during each phase (−50 – +50 VAS "How do you perceive this geometric figure?", anchors: −50 = very pleasant, 0 = neutral, 50 = very unpleasant).

Table 1 | Noxious stimulation

	Decrease (VAS0)	Medium (VAS40)	Increase (VAS80)
Applied temperature level (in °C)			
Mean (*SD*)	25.00 (4.59)	38.90 (4.86)	40.30 (4.99)
Median [Min, Max]	24.60 [20.0, 35.0]	39.90 [30.0, 45.0]	41.30 [30.6, 47.3]
Pain intensity: acquisition			
Mean (*SD*)	9.51 (11.10)	37.90 (20.00)	77.60 (14.40)
Median [Min, Max]	6.17 [0.0, 44.3]	39.00 [1.0, 83.0]	79.70 [22.0, 99.0]
Pain (un)pleasantness: acquisition			
Mean (*SD*)	−29.90 (16.90)	5.20 (13.90)	30.90 (12.10)
Median [Min, Max]	−32.80 [−50.0, 10.0]	5.80 [−36.3, 34.7]	32.70 [3.3, 50.0]
Pain intensity: extinction			
Mean (*SD*)	–	27.40 (17.40)	–
Median [Min, Max]	–	25.80 [0.0, 70.4]	–
Pain (un)pleasantness: extinction			
Mean (*SD*)	–	−1.88 (17.20)	–
Median [Min, Max]	–	1.60 [−50.0, 26.0]	–

Data are provided based on $n = 68$ participants.

Differential valence ratings, reflecting learning at the affective level relative to the control condition, significantly changed over the course of acquisition training in both conditions (*time*: $\beta = 4.55$, $F(1, 461.29) = 53.48$, $p < 0.001$; Fig. 2b). Relative to the control condition, neither the slope nor the absolute level differed between the aversive and the appetitive condition (*CS type*: $F(1, 163.61) = 0.43$, $p = 0.512$; *CS type* x *time*: $F(1, 459.31) = 1.66$, $p = 0.199$; Fig. 2b). To explore whether this finding was due to any changes in the control condition, we also analysed valence ratings separately for each of the three conditions (Fig. 2c). This model revealed a significant interaction between *CS type* and *time* ($F(2, 751.77) = 54.00$, $p < 0.001$). While valence ratings increased for the $CS_{increase}$ ($p < 0.001$, detailed statistics for all post-hoc tests can be found in Table 2), they decreased for the $CS_{decrease}$ ($p < 0.001$). Pairwise comparisons showed that slopes for the reinforced CS differed significantly from the CS_{medium} ($CS_{increase} > CS_{medium}$, $p < 0.001$; $CS_{decrease} < CS_{medium}$, $p < 0.001$). Valence ratings also increased slightly for the CS_{medium} ($p = 0.010$). These results indicate acquisition learning for both reinforced CS types, but also a small change in valence of the non-reinforced CS_{medium}. An exploratory direct comparison of the $CS_{increase}$ and $CS_{decrease}$ showed that their individual slopes differed significantly (two-sided paired *t*-test on individual slopes with slopes for $CS_{decrease}$ calculated as x (−1) for direct comparison, $CS_{inccease} > CS_{decrease}$, $t(67) = -2.23$, $p = 0.029$, $d = 0.27$). This finding further indicates that changes in valence ratings were more pronounced in the aversive than the appetitive condition.

As shown in Fig. 2c, valence ratings were rapidly adjusted early in the acquisition phase. To investigate this initial learning further, we applied a linear model to compare changes in valence ratings from habituation to the first reinforced acquisition trial (A1-H0) by *CS type*. This exploratory analysis revealed a significant main effect of *CS type* ($F(2,173) = 12.43$, $p < 0.001$). Specifically, while the $CS_{increase}$ already significantly differed from the CS_{medium} ($p < 0.001$), the $CS_{decrease}$ did not ($p = 0.694$; Fig. 2d), indicating that participants made stronger early adjustments to their ratings in the aversive than the appetitive condition and therefore providing evidence for asymmetric acquisition.

CS-US contingency ratings. Contingency ratings were obtained after acquisition and extinction training ("How often was this geometric figure followed by a painful stimulus?", anchors: −100 = "100% cold stimulus", 0 = "no change", 100 = "100% heat stimulus"). Ratings for the $CS_{decrease}$ were flipped for analyses. The analysis of CS-US contingency ratings as a complementary measure to CS valence showed a significant interaction of *CS type* and *timepoint* ($F(2, 335) = 6.28$, $p = 0.002$; Fig. 2e). After acquisition training, contingency ratings for the $CS_{increase}$ and the $CS_{decrease}$ were significantly increased in the expected direction relative to the CS_{medium} ($CS_{increase} > CS_{medium}$, $p < 0.001$; $CS_{decrease} > CS_{medium}$, $p < 0.001$).

Extinction

Valence ratings. During extinction, differential valence ratings decreased across conditions (*time*: $\beta = -3.59$, $F(1, 366.12) = 40.44$, $p < 0.001$), but the decrease did not differ between *CS types* (*CS type* x *time*: $F(1, 365.37 = 0.86$, $p = 0.353$; Fig. 2b). To test whether this finding could be explained by a change in the control condition, we analysed the valence ratings of all three conditions separately (Fig. 2c). While both $CS_{increase}$ and $CS_{decrease}$ showed a change in valence ratings towards the expected direction (i.e., decreasing ratings in $CS_{increase}$ and increasing ratings for $CS_{decrease}$), valence ratings for the CS_{medium} did not change significantly ($p = 0.997$). An exploratory direct comparison of the $CS_{increase}$ and $CS_{decrease}$ showed that individual slopes did not differ between CS types (two-sided paired *t*-test on individual slopes, slopes for $CS_{decrease}$ value x (−1), $t(67) = -1.14$, $p = 0.257$, $d = 0.14$). In line with the analysis of initial acquisition, we next performed an additional linear model on the difference of the last acquisition rating and the first extinction rating across conditions as a measure for initial

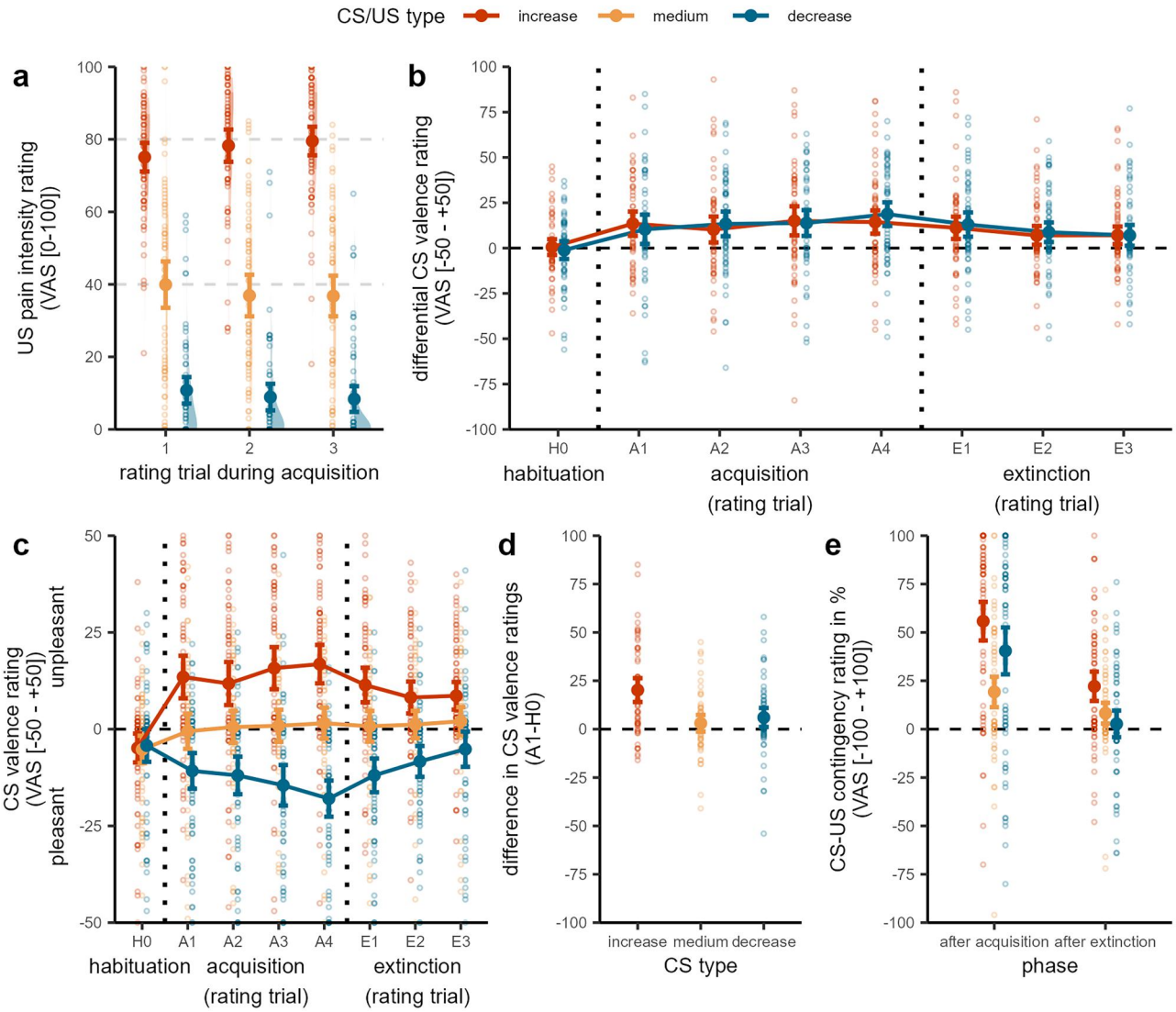


Fig. 2 | Behavioural results. Condition-wise means (dark-coloured dots) and 95% confidence intervals (error bars) are displayed, along with individual data points (light colours). Data are provided for $n = 68$ participants. Analyses were carried out using a linear mixed model in (**a**–**c**) and (**e**), and a linear model in (**d**). Each was followed by post-hoc tests with adjustment for multiple comparisons. Tests were carried out two-sided. **a** US pain intensity ratings (0–100 VAS "How painful was this temperature stimulus?") for the $US_{increase}$ and the $US_{decrease}$ were significantly different from the control condition (US_{medium}). **b** Differential valence ratings of $CS_{increase/decrease}$ relative to the CS_{medium} did not differ between conditions during acquisition (A1–A4) or extinction (E1–E3). **c** Valence ratings (−50 – +50 VAS "How do you perceive this geometric figure?") of all three conditions ($CS_{increase}$, $CS_{decrease}$ and CS_{medium}). Note that positive values indicate an unpleasant perception and negative values indicate a pleasant perception. **d** Early acquisition learning, defined as the difference in valence rating between the first acquisition rating (A1) and the habituation rating (H0), was most pronounced in the aversive (increase) condition. **e** CS-US contingency ratings (−100 = "100% cold stimulus", 0 = "no change", 100 = "100% heat stimulus" VAS "How often was this geometric figure followed by a painful stimulus?"), with positive values reflecting correct contingency learning for the $CS_{increase/decrease}$, i.e., value x (−1) for the $CS_{decrease}$. CS conditioned stimulus, US unconditioned stimulus, VAS visual analogue scale.

extinction. Here, comparing the aversive and appetitive conditions showed no significant difference in initial extinction strength ($F(2,182) = 2.07$, $p = 0.129$) supporting the main analysis of extinction slopes.

Further, an exploratory comparison of valence ratings during habituation with ratings obtained at the end of the extinction phase showed that the acquired CS-US associations were not extinguished similarly for the pain and pain relief condition. While valence ratings for the $CS_{decrease}$ returned to the baseline level after extinction ($p = 0.963$), they were still significantly higher after extinction as compared to the habituation phase for the $CS_{increase}$ ($p < 0.001$), indicating incomplete extinction for aversive pain-related learning. This result further provides evidence of asymmetric extinction between the aversive and appetitive conditions.

CS-US contingency ratings. Contingency ratings for both $CS_{increase}$ and $CS_{decrease}$ decreased significantly from after acquisition to after extinction training (extinction - acquisition: $CS_{increase}$, $p < 0.001$; $CS_{decrease}$, $p < 0.001$). However, the change of the $CS_{increase}$ and the $CS_{decrease}$ did not differ significantly ($p = 0.979$).

When directly comparing the level of contingency, ratings were higher for the increase condition than for the decrease condition at both time points (after acquisition, $p = 0.021$; after extinction, $p = 0.002$). While after extinction training, the $CS_{increase}$ still differed from the CS_{medium} ($CS_{increase}$ > CS_{medium}, $p = 0.043$), the $CS_{decrease}$ and CS_{medium} did no longer differ significantly ($p = 0.604$). Importantly, the $CS_{increase}$ remained significantly different from zero after extinction training ($p < 0.001$), while the CS_{medium} ($p = 0.159$) and the $CS_{decrease}$ did not ($p = 0.893$), indicating incomplete extinction for contingency ratings for the aversive condition.

Table 2 | Results of learning-related post-hoc tests

Contrast	Estimate	*CI*	*SE*	*n*	*df*	*t*-ratio	$p_{adjusted}$
CS valence acquisition training							
CS type x time							
$slope_{time}$ CS_{i-d}	7.78	[6.02, 9.55]	0.75	68	751	10.35	< 0.001***
$slope_{time}$ CS_{i-m}	3.12	[1.37, 4.87]	0.75	68	749	4.19	< 0.001***
$slope_{time}$ CS_{m-d}	4.66	[2.88, 6.45]	0.76	68	753	6.14	< 0.001***
CS type x time – vs. zero							
CS_i	4.69	[3.44, 5.94]	0.52	68	746	9.00	< 0.001***
CS_m	1.57	[0.30, 2.85]	0.53	68	751	2.96	0.010*
CS_d	−3.09	[−4.39, −1.79]	0.54	68	755	-5.70	< 0.001***
CS valence initial acquisition learning							
CS type							
CS_{i-d} acq	14.15	[5.54, 22.77]	3.64	66	173	3.88	< 0.001***
CS_{i-m} acq	17.15	[8.42, 25.88]	3.69	67	173	4.65	< 0.001***
CS_{d-m} acq	3	[−5.69, 11.69]	3.68	66	173	0.82	0.694
Contingency acquisition							
CS type							
CS_{i-m}	36.56	[23.04, 50.08]	5.74	68	335	6.37	< 0.001***
CS_{d-m}	21.21	[7.69, 34.73]	5.74	68	335	3.69	< 0.001***
CS_{i-d}	15.35	[1.83, 28.87]	5.74	68	335	2.67	0.021*
CS valence extinction training							
CS type x time							
$slope_{time}$ CS_i	−2.77	[−3.98, −1.57]	0.50	68	572	-5.51	< 0.001***
$slope_{time}$ CS_m	0.09	[−1.13, 1.31]	0.51	68	574	0.18	0.997
$slope_{time}$ CS_d	4.02	[2.75, 5.28]	0.53	68	576	7.61	< 0.001***
CS valence incomplete extinction learning							
CS type x time							
CS_i E3-H	13.53	[7.42, 19.65]	2.55	68	319	5.32	< 0.001***
CS_m E3-H	7.26	[1.05, 13.47]	2.59	68	321	2.81	0.016*
CS_d E3-H	-1.13	[-7.45, 5.19]	2.63	68	323	-0.43	0.963
Contingency extinction							
CS type x time							
CS_i ext-acq	−33.68	[−48.06, −19.29]	5.74	68	335	−5.86	< 0.001***
CS_m ext-acq	−11	[−25.38, 3.38]	5.74	68	335	−1.92	0.207
CS_d ext-acq	−37.71	[−52.09, −23.32]	5.74	68	335	−6.57	< 0.001***
CS_{i-d} ext-acq	4.03	[−16.31, 24.37]	8.12	68	335	0.50	0.979
CS_{i-m} ext	13.88	[0.36, 13.88]	5.74	68	335	2.42	0.043*
CS_{d-m} ext	−5.5	[−19.02, 8.02]	5.74	68	335	−0.96	0.604
CS_{i-d} ext	19.38	[5.86, 32.90]	5.74	68	335	3.38	0.002**
CS type x time – vs. zero							
CS_i ext	22.12	[11.81, 32.42]	4.3	68	380	5.15	< 0.001***
CS_m ext	8.24	[−2.07, 18.54]	4.3	68	380	1.92	0.159
CS_d ext	2.74	[−7.57, 13.04]	4.3	68	380	0.64	0.893

Post-hoc tests with adjustment for multiple comparisons following up on the respective linear mixed models based on the number of participants as stated within the table, all tests were carried out two-sided.
CS conditioned stimulus, *i* increase, *d* decrease, *m* medium, *CI* confidence interval, *SE* standard error, *df* degrees of freedom, $p_{adjusted}$ adjusted *p*-value.

Neuroimaging results

The primary neuroimaging analyses addressed the main research question of common and distinct neural activation patterns of aversive and appetitive learning (modelled as *time* x *condition* interactions). All subsequent analyses, including gPPI analyses and analyses of incomplete extinction, were considered exploratory.

Acquisition phase: common neural responses during aversive and appetitive learning

To identify brain regions in which activation changed over time in both aversive and appetitive acquisition, we conducted a conjunction analysis ($[CS_{increase\ x\ time} - CS_{medium\ x\ time}] \cap [CS_{decrease\ x\ time} - CS_{medium\ x\ time}]$). A joint activation increase was found in the occipital cortex, primarily

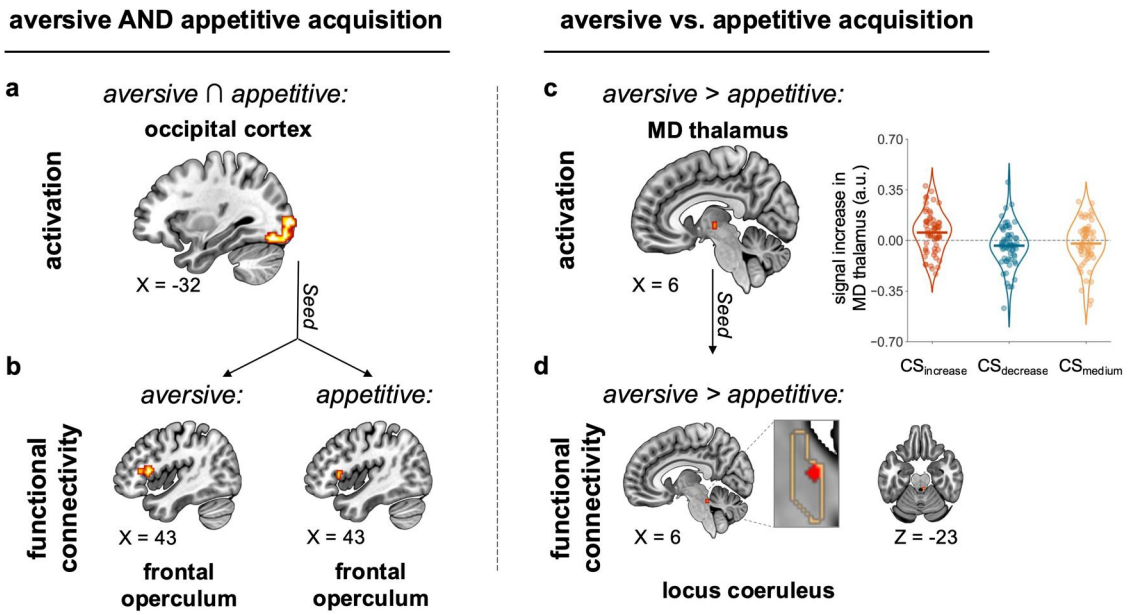


Fig. 3 | Joint and distinct activation and functional connectivity during CS events in the acquisition phase. a Brain regions showing a significant activation increase during both aversive (pain increase) and appetitive (pain relief) acquisition. **b** Functional connectivity of the cluster in the occipital cortex separately for both types of learning. **c** The right mediodorsal (MD) thalamus showed a stronger activation increase during aversive than appetitive acquisition. The inset displays parameter estimates (in arbitrary units) for each of the three conditions. **d** The cluster in the right MD thalamus showed a stronger increase in functional connectivity with the right locus coeruleus during aversive than appetitive learning. The middle inset overlaid the activation cluster with the locus coeruleus mask (shown in contour)[61]. a.u. arbitrary units.

encompassing visual areas V4 and V3 ($t = 5.11$, $p_{\text{cluster-FWE}} < 0.001$; Fig. 3a, Supplementary Table S2). No brain regions showed a significant decrease in activation. To further investigate these findings, we examined the functional connectivity of the activated brain cluster during aversive and appetitive learning. Using the activated cluster in the occipital cortex as a seed region, we found increased positive coupling over time with the frontal operculum in both conditions (aversive: $t = 4.21$, $p_{\text{SVC-FWE}} = 0.011$, $k_E = 7$, MNI coordinates: [43,19,8]; appetitive: $t = 3.80$, $p_{\text{SVC-FWE}} = 0.036$, $k_E = 5$, MNI coordinates: [43,19,5]; Fig. 3b). This result suggests a synchronised increase in activity over time in the occipital cortex and frontal operculum, independent of CS valence.

Acquisition phase: distinct neural responses of aversive and appetitive learning

When directly comparing the appetitive and the aversive condition (contrast: $[CS_{\text{increase x time}} - CS_{\text{medium x time}}] > [CS_{\text{decrease x time}} - CS_{\text{medium x time}}]$), the aversive condition induced a stronger signal increase in the right thalamus over the course of acquisition, specifically in the mediodorsal (MD) nucleus ($t = 4.06$, $p_{\text{SVC-FWE}} = 0.042$; Fig. 3c, Supplementary Table S2). No significant result was found for the opposite contrast testing a stronger increase in activation in the appetitive condition ($[CS_{\text{decrease x time}} - CS_{\text{medium x time}}] > [CS_{\text{increase x time}} - CS_{\text{medium x time}}]$).

Using the identified MD thalamus cluster as a seed region, we investigated the functional connectivity of this cluster during differential learning over time ($[CS_{\text{increase x time}} - CS_{\text{medium x time}}] > [CS_{\text{decrease x time}} - CS_{\text{medium x time}}]$). This analysis revealed a stronger increase over time in positive connectivity with the right locus coeruleus (LC; $t = 3.26$, $p_{\text{SVC-FWE}} = 0.018$, $k_E = 1$, MNI coordinates: [6,−38,−23]; Fig. 3d), indicating a stronger increase in MD thalamus - LC coupling over the acquisition phase in the aversive than the appetitive condition.

Extinction phase: common neural responses of aversive and appetitive learning

A conjunction analysis testing a common signal decrease during extinction ($[CS_{\text{increase x time}} - CS_{\text{medium x time}}] \cap [CS_{\text{decrease x time}} - CS_{\text{medium x time}}]$) revealed that no cluster survived the threshold of $p_{\text{SVC-FWE}} < 0.05$, while the ventromedial prefrontal cortex (vmPFC) showed a trend-level decrease in response in both conditions ($t = 3.39$, $p_{\text{SVC-FWE}} = 0.063$; Fig. 4a, Supplementary Table S3). No regions exhibited shared increasing activities across the two conditions.

Extinction phase: distinct neural responses during aversive and appetitive learning

In the next step, we also compared the two conditions (both relative to the CS_{medium} condition). The contrast ($[CS_{\text{decrease x time}} - CS_{\text{medium x time}}] > [CS_{\text{increase x time}} - CS_{\text{medium x time}}]$) revealed a greater decrease in activation in the parahippocampal gyrus (PHG) during extinction in the appetitive condition compared to the aversive condition ($t = 4.02$, $p_{\text{SVC-FWE}} = 0.041$; Fig. 4b, Supplementary Table S3). The reverse contrast ($[CS_{\text{increase x time}} - CS_{\text{medium x time}}] > [CS_{\text{decrease x time}} - CS_{\text{medium x time}}]$) yielded no significant result. To further investigate the differential engagement of the PHG, we conducted a connectivity analysis using the identified cluster as a seed region. However, the search for brain regions showing a stronger decrease over time in functional connectivity with the PHG extinction showed no significant result.

Residual anticipatory activity during the late CS phase as correlate of incomplete extinction

To investigate the neural basis of incomplete aversive extinction which we had also found previously[15], we investigated activations during the late CS phase before US delivery as a proxy of (residual) pain anticipation[19]. To limit this search to brain regions involved in learning, we identified areas showing an activation increase during acquisition ($[CS_{\text{increase x time}} - CS_{\text{medium x time}}]$) that also showed an activation decrease during extinction relative to the control condition ($[CS_{\text{increase x time}} - CS_{\text{medium x time}}]$). During aversive acquisition ($[CS_{\text{increase x time}} - CS_{\text{medium x time}}]$), late CS presentation was accompanied by a signal increase in a left occipital cortex cluster at whole-brain correction level ($t = 4.07$, $p_{\text{cluster-FWE}} = 0.029$, $k_E = 64$, MNI coordinates: [−27,−93,−11]). Notably, the same occipital region also exhibited a signal decrease during the extinction phase ($t = 4.25$, $p_{\text{SVC-FWE}} = 0.002$, $k_E = 4$, MNI coordinates: [−32,−90,−17]; Fig. 5a), indicating its involvement in both learning phases. Parameter estimates

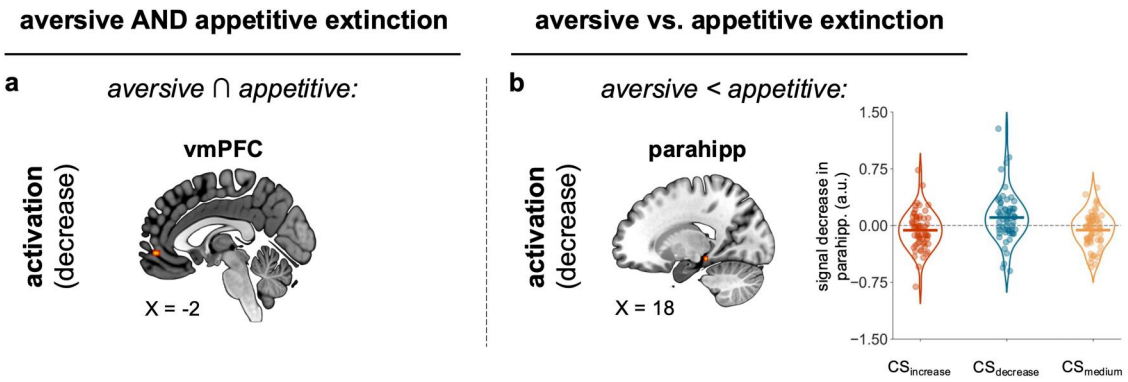


Fig. 4 | Joint and distinct activation and functional connectivity during CS events in the extinction phase. a The vmPFC showed a trend-level activation decrease during both aversive (pain increase) and appetitive (pain relief) extinction learning. **b** The parahippocampal gyrus displayed stronger activation decrease in the appetitive than the aversive condition. The inset displays parameter estimates (in arbitrary units) for each of the three conditions. vmPFC ventromedial prefrontal cortex, parahipp parahippocampal gyrus, a.u. arbitrary units.

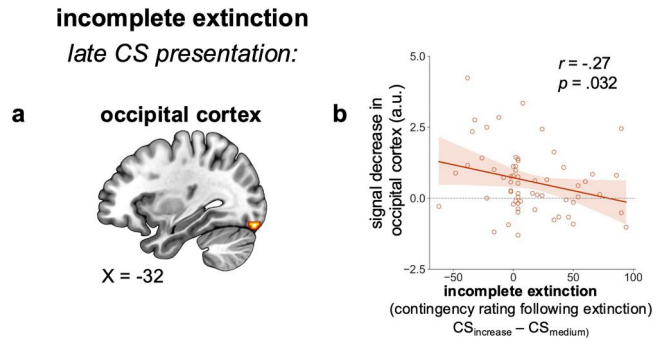


Fig. 5 | Occipital cluster involved in learning shows residual engagement during (anticipatory) late CS phase related to incomplete extinction. a The left occipital cortex showed an activation increase during acquisition [$CS_{increase\ x\ time} - CS_{medium\ x\ time}$] and an activation decrease during extinction in the late phase of aversive (pain increase) CS presentation [$CS_{increase\ x\ time} - CS_{medium\ x\ time}$], indicating its involvement in learning across phases. **b** The same occipital cluster showed residual activation in the late CS phase, with greater activation corresponding to more incomplete extinction in the aversive condition (as indicated by contingency ratings). Association was tested with Pearson's correlation (two-tailed; $n = 61$). The solid line shows the linear relationship between the two measures, with the shaded band indicating the 95% confidence interval and open circles representing individual participants. CS conditioned stimulus; a.u. arbitrary units.

extracted from this occipital cortex cluster showed a negative correlation with our behavioural index of incomplete extinction in the aversive condition (i.e., difference in contingency rating between $CS_{increase}$ and CS_{medium} following extinction) ($r = -0.27$, $p = 0.032$; Fig. 5b). This indicates that incomplete extinction in the aversive condition is linked to residual anticipatory engagement in the occipital lobe shortly before the US is presented. No significant result was found in other brain regions.

Discussion

This study compared aversive and appetitive pain-related learning during acquisition and extinction at both behavioural and neural levels within the same experimental paradigm. Key findings were: (1) In a direct comparison of pain exacerbation (aversive) and pain relief (appetitive) learning, early changes in valence ratings and elevated valence ratings after extinction for pain exacerbation suggest stronger initial adjustments in aversive acquisition learning as well as incomplete extinction of cue–pain associations. Contingency ratings, reflecting cognitive aspects of learning, corroborate these findings indicating increased acquisition and incomplete extinction in the aversive condition. (2) Neuroimaging analyses suggested shared increases in visual cortex activity during appetitive and aversive acquisition and a trend-level decrease in vmPFC activity during appetitive and aversive extinction. (3) They further suggested greater MD thalamus activation and stronger functional connectivity over time with the LC during aversive compared with appetitive acquisition. (4) Aversive extinction showed a weaker activation decrease in the PHG than appetitive extinction. (5) Incomplete cognitive aversive extinction scaled with residual visual cortex activity during the late CS phase linked to US anticipation.

As indicated by valence and contingency ratings, participants demonstrated enhanced acquisition learning for pain exacerbation than for pain relief cues. Moreover, the exploratory post-hoc analysis of initial learning revealed more pronounced effects for the $CS_{increase}$, indicating fast adaptation to aversive pain-related learning. Although valence ratings suggested that extinction learning occurred at a comparable pace in both conditions, a complementary comparison of ratings obtained at the beginning and end of the task revealed an intriguing difference between both conditions. At the end of the extinction phase, valence and contingency ratings had returned to pre-acquisition levels in the pain relief condition. However, they remained elevated in the pain increase condition, suggesting incomplete extinction on both affective and cognitive dimensions of pain-related learning. This persistence of aversive cue–pain associations replicates findings from van der Schaaf and colleagues using the same paradigm[15] and is consistent with broader evidence that aversive associations can be acquired more rapidly and extinguish less completely than associations linked to safety or reward[18]. Although the paradigm aimed to achieve approximately equidistant pain calibration, this could not be fully maintained throughout the experiment due to habituation and interindividual variability.

To investigate the potential neural mechanisms underlying these behavioural differences, we next examined joint and distinct brain activations during pain and pain relief learning. Specifically, we investigated how neural activity and functional connectivity patterns evolve across acquisition and extinction, shedding light on the differential processing of aversive and appetitive cues.

During acquisition, both learning types showed significant signal increases in the occipital lobe, specifically within visual areas V3 and V4, in response to the conditioned stimulus. This occipital activation occurred prior to temperature modulation, suggesting increased visual cortical engagement during anticipation of the stimulus change. Previous work suggests that visual cortex activity increases in anticipation of behaviourally relevant events, a process sometimes described as preparatory attention, whereby neural populations in sensory cortex are more engaged in expected inputs[20–22]. While our design did not include an independent manipulation or behavioural measure of attention, the timing of the effect is consistent with anticipatory modulation of visual processing during learning.

This interpretation is further supported by our gPPI findings. Increased functional connectivity between the occipital cortex and frontal operculum emerged during both aversive and appetitive learning. The frontal operculum has been implicated in fear learning across experimental paradigms[9,23] and, together with the inferior frontal junction, in top-down modulation of visual cortex during anticipation of behaviourally relevant events. In our paradigm, CS offset coincided with a change in visual input (Fig. 1b), shortly after the onset of temperature change (i.e., pain increase/decrease). Because the visual display (black screen) was identical across conditions, this change likely functioned as a general signal indicating an impending temperature shift rather than conveying directional information about the upcoming stimulus. The observed occipital–operculum coupling (Fig. 3b) is therefore compatible with learning-related modulation of visual processing rather than visual processing per se. However, the small cluster size warrants cautious interpretation, and the present data do not allow conclusions about the direction of information flow or the precise functional role of this interaction.

When comparing pain and relief learning, we observed that the right MD thalamus showed increased activation upon presentation of the visual cue signalling pain increase (Fig. 3c). The MD thalamus plays a crucial role in aversive learning through its connections with the amygdala and prefrontal regions, facilitating the integration of sensory and affective information essential for forming aversive memories that guide future behaviour and the execution and control of higher-level cognitive functions[24,25]. Additionally, the MD thalamus is well-connected to key attention-related regions, including the anterior cingulate cortex supporting its role in prioritising relevant incoming information.

The stronger functional connectivity between the MD thalamus and the noradrenergic LC over time during aversive pain-related learning may indicate greater engagement of subcortical systems associated with arousal and the prioritization of behaviourally relevant information[26,27]. The MD thalamus receives diverse inputs from brainstem structures, including the LC and substantia nigra, with a topographical organisation[28]. The LC is a major source of noradrenaline and regulates alertness and arousal. Thus, the observed increase in coupling is consistent with enhanced processing of behaviourally salient stimuli during cues predicting pain exacerbation. However, given that this ROI finding was based on a very small cluster, it should be interpreted cautiously. Moreover, the present design does not allow to determine whether this interaction specifically reflects threat-related processing or more general arousal or salience mechanisms.

Together, these findings suggest that aversive and appetitive pain-related acquisition learning engage both shared and distinct neural mechanisms during acquisition. Although the acquisition of appetitive and aversive learning has been investigated in numerous studies[29–32], we here directly compare the temporal dynamics of neural responses during the acquisition of appetitive and aversive pain-related associations within the same individuals. In a seminal study, Seymour and colleagues examined both pain and relief acquisition learning within the same participants and identified distinct appetitive and aversive prediction-error signals alongside shared responses in the ventral striatum and anterior insula[14]. However, their analyses focused on model-derived appetitive and aversive prediction-error signals during ongoing probabilistic learning rather than on the behavioural and neural dynamics of acquisition. Thus, rather than being directly comparable, the two studies provide complementary insights into appetitive and aversive pain-related learning, with Seymour et al. characterising computational teaching signals during probabilistic learning and the present study examining how neural responses evolve over the course of acquisition and extinction. Importantly, our findings suggest that the behavioural asymmetry between aversive and appetitive learning is paralleled by differences in how neural responses develop over the course of learning. While both forms of learning showed increasing occipital responses and occipital-opercular connectivity across acquisition, aversive learning was characterised by a stronger increase in MD thalamic responses and, in exploratory analyses, MD-LC connectivity. This pattern is consistent with greater recruitment of neural processes implicated in attentional prioritisation and arousal as aversive learning progresses.

During extinction, both aversive and appetitive extinction shared a trend-level signal decrease over time in the vmPFC (Fig. 4a), a key region widely implicated in fear extinction across humans and animal studies[33–35]. Notably, extinction is temporally sensitive[36] and as Morriss and colleagues[37] commented, a more statistically powerful approach should be employed such as applying time modulators to regressors to capture linear changes over time[38,39]. Following these suggestions, our analysis revealed a trend towards temporal changes in vmPFC activity that did not differ between aversive and appetitive extinction.

The direct comparison of pain-related appetitive and aversive extinction learning revealed a weaker signal decrease in the right PHG during the aversive condition (Fig. 4b). The observed pattern is compatible with previous evidence implicating the PHG in contextual associative processing and memory retrieval, particularly in situations where previously learned stimulus-outcome relationships are updated or evaluated[40]. Although speculative at this point, one tentative interpretation is that the weaker signal decline during aversive extinction is associated with sustained engagement of contextual memory processes when cues predict a potential increase in pain. In contrast, the stronger PHG decrease during appetitive extinction may indicate a more rapid disengagement of contextual representations associated with pain relief.

To further explore the neural underpinnings of incomplete extinction suggested by contingency ratings in more detail, we conducted an additional analysis focusing specifically on the late phase of CS presentation, a period when participants begin anticipating the US, as suggested by Eippert and colleagues[19]. This approach allows us to capture anticipatory processes that may differ between appetitive and aversive conditions, such as pain and pain relief learning. If extinction learning in the aversive condition is indeed incomplete, as indicated by our contingency data analysis, we would expect sustained activation in regions associated with pain anticipation, reflecting the persistence of conditioned threat responses. The analysis revealed that incomplete extinction was related to a lesser decrease in occipital cortex activity during extinction (Fig. 5). In line with the notion of preparatory attention discussed above, the weaker signal decrease in the visual cortex during extinction in the aversive relative to the control condition may suggest sustained anticipatory processing of the expected stimulus outcome. While common visual processing is cancelled out in the differential neural contrasts, the present paradigm may not fully disambiguate learning-related modulation of visual cortex from a residual contribution of low-level visual processing.

Together, these findings suggest that the behavioural asymmetry between aversive and appetitive pain-related learning is paralleled by neural asymmetries across acquisition and extinction, which may also have translational relevance. In chronic pain, expectations about whether pain will worsen or improve can influence behaviour and treatment outcomes. A tendency to preferentially acquire associations signalling pain exacerbation and retain these associations when contingencies change could contribute to persistent expectations of worsening pain. Our findings identify candidate neural processes associated with this asymmetry that can now be examined in clinical pain populations.

Several limitations should be considered when interpreting these findings. First, although the present findings may reflect general principles of aversive and appetitive learning, the exclusive use of an experimental pain model does not allow us to determine whether the observed effects are pain-specific, generalise across sensory modalities, or reflect domain-general mechanisms of aversive and appetitive learning. In addition, no significant skin conductance responses to CS were observed during acquisition or extinction. Although these analyses were based on a substantially reduced sample due to technical issues ($n = 27$), the findings indicate that the learning effects observed in subjective ratings were not corroborated by the physiological measure assessed in this study (see

Supplementary physiological analyses and Supplementary physiological results). Second, habituation to prolonged tonic heat stimulation resulted in a gradual reduction of overall pain. However, all conditioned stimuli were experienced within the same evolving context, allowing comparisons between aversive, appetitive, and reference conditions. Third, the ROI findings based on small significant clusters as well as the use of multiple individual SVC analyses require that the neuroimaging results should be considered with caution. Finally, although our experimental paradigm successfully induced pain amplification and relief in a tonic pain context designed to mimic aspects of clinical pain, it remains a controlled, artificial model. Chronic pain is a complex, multi-faceted experience, shaped by biological, psychological and social factors and caution is therefore warranted in extrapolating these findings to chronic pain populations. This is particularly relevant given that we did not observe reliable associations between neural measures and individual behavioural indices of learning, which may partly reflect the modest behavioural effect sizes and limited variability in some of the behavioural measures. Future research should establish the behavioural relevance of these neural processes, for example through trial-by-trial modelling of learning signals.

In summary, our behavioural findings provide evidence that aversive pain-related associations are acquired more readily and extinguish less completely than appetitive associations. Exploratory neuroimaging findings were consistent with the behavioural evidence for incomplete aversive extinction, primarily in the occipital cortex and PHG. These neuroimaging analyses suggest that these behavioural asymmetries may be accompanied by partly overlapping and partly distinct neural processes involving visual cortex, MD thalamus, PHG, and other learning-related regions. These findings point towards candidate neural mechanisms that may contribute to the persistence of aversive cue–pain associations. Such asymmetries in aversive versus appetitive learning have been proposed as contributing factors in the persistence of threat-related expectations in conditions such as chronic pain and anxiety disorders.

Methods

Participants

A total of $N = 84$ healthy, right-handed participants were recruited through advertisements. Exclusion criteria were age <18 or >75 years, a self-reported history of acute or chronic pain or other neurological or psychiatric disorders, regular use of medication (including hormonal contraception), contraindication to MRI scans, pregnancy or breastfeeding, allergy to capsaicin, acute sunburn or other dermatological abnormalities on the volar forearm, BMI > 30 or <18, and left-handedness. Demographic information was collected via self-reports (Supplementary Table S1). Socioeconomic status, communities of descent or race/ethnicity are unavailable.

Data from $n = 16$ participants were excluded from the behavioural analyses due to pain intensity not being perceived as intended ($n = 9$), early termination of the experiment by the participants ($n = 3$) and technical errors ($n = 4$). Thus, behavioural analyses included $n = 68$ participants ($n_{male} = 33$, $n_{female} = 35$, mean age = 37.65 ± 13.19 years), while fMRI analyses are based on $n = 61$ participants ($n_{male} = 31$, $n_{female} = 30$, mean age = 37.51 ± 13.28 years; $n = 7$ participants were excluded from the fMRI analysis due to missing data).

Participants gave written informed consent before the start of the experiment and received a monetary compensation for their participation (50 Euro plus 15 Euro/hour). The study was registered at the German register for clinical trials (https://www.drks.de/search/de/trial/DRKS00027448/details) on February 1, 2022 during the data collection process as part of a broader study framework, including the general study design, experimental paradigm, and primary methodological framework. Detailed research aims, hypotheses, analysis plans or ROIs were not specified in the initial registration. The study was approved by the local Ethics Committee (16-7248-BO) of the Medical Faculty, University Duisburg-Essen in accordance with the Declaration of Helsinki. Participants could withdraw from the study at any time.

Experimental procedures and paradigm

Please note that the experimental paradigm and study procedures were highly similar to those used in our behavioural prestudy[15]. However, both studies were conducted entirely independently, and there was no overlap in participants.

The study was conducted over two experimental days (mean number of interval days = 2.31, range [0, 4]). On day 1, participants underwent a calibration procedure to determine the individual temperature levels for the thermal stimuli and completed several questionnaires to collect demographic information and assess psychological variables (see Supplementary Methods Questionnaires).

On day 2, participants completed additional psychometric questionnaires after the capsaicin cream was again applied. Approximately 45 min later, participants were positioned in the MRI scanner and their heat pain thresholds were reassessed (see Supplementary Methods Temperature calibration). Participants then completed the conditioning task in the MRI scanner (see Differential conditioning paradigm), followed by high-resolution whole-brain T1-weighted and DTI scans. Note that only task-based fMRI results are reported here. DTI results will be reported elsewhere.

Differential conditioning paradigm

The differential conditioning paradigm comprised a habituation, acquisition and extinction learning phase. During both the acquisition and the extinction phases, individually calibrated contact heat stimuli (unconditioned stimuli, US; see Noxious thermal stimulation) were paired with predictive visual cues (conditioned stimuli, CS; see Visual cues) (Fig. 1). Moderate heat stimuli were continuously applied to induce the ongoing tonic pain throughout the experiment. The CS-US association was examined in three experimental phases: habituation (CS familiarization), acquisition training (CS presentation; 75% US reinforcement rate) and extinction training (CS presentation; no reinforcement). Before the experiment, participants were informed about the potential CS-US association in the acquisition and extinction phases, though they were not given details about the actual contingency. The assignment of the geometric figures to the CS conditions was balanced and pseudo-randomized across participants, i.e., a comparable number of participants received the square, rectangle and rhombus as $CS_{increase}$, CS_{medium} and $CS_{decrease}$, respectively. The exact distribution can be found in Supplementary Table S4.

Habituation. During habituation, each CS was presented three times without any change in temperature (US_{medium}).

Acquisition training. During acquisition training, a total of 48 CS was presented (16 per type). The $CS_{increase}$ and $CS_{decrease}$ were each paired with their corresponding US ($US_{increase}$ and $US_{decrease}$) at a 75% reinforcement rate, resulting in 12 reinforced CS per type. The CS_{medium} was followed by no change in temperature (US_{medium}), therefore serving as a stable reference condition to account for unspecific changes in ratings over time (e.g., habituation, sensitization). The first and last trials of each condition were reinforced to ensure reliable establishment of the CS-US association at the beginning of acquisition and to minimize potential extinction effects toward the end of the acquisition phase. This approach follows previous work using the same paradigm[15]. Because only two trials per condition were fixed in this way while all remaining trials followed a probabilistic reinforcement schedule, this manipulation was unlikely to introduce meaningful predictability for participants.

Extinction training. Following the acquisition training, no additional instructions were provided. During extinction training, 36 CS (12 per type) were presented with US_{medium} only (i.e., ongoing thermal stimulation with temperature corresponding to VAS40). Importantly, because all CS types were followed by the same US_{medium}, extinction training eliminated the previously learned CS-US contingencies during acquisition without introducing the new differential associations, while

preserving the ongoing tonic pain context, consistent with a standard extinction procedure[41,42].

Trial structure. On each trial, the CS was presented for 9 s, followed by a black screen for 10.5 s. The US were applied for 8 s, starting 1.5 s before the offset of the CS (i.e., CS and US overlapped for 1.5 s), with a 6.5 s overlap with the presentation of the black screen. A white fixation cross was displayed during the inter-trial-intervals (ITI) that were jittered between 6 and 11 s. The 1.5-s overlap between the conditioned stimulus (CS) and unconditioned stimulus (US) was chosen to maintain a delay-conditioning procedure, which is considered more effective than trace conditioning for establishing robust conditioned associations[43], and to ensure that, given the gradual onset of thermal pain, participants began to experience the pain stimulus while the predictive cue was still present[44].

During acquisition training, CS were displayed in a pseudo-randomized order (see Supplementary Table S5 for the 6 pre-defined orders), ensuring that (1) the same CS type was presented no more than three times consecutively and (2) each CS type was equally distributed across both halves of the experimental phases, i.e., first and second half of the acquisition and extinction phases, respectively. This resulted in 8 CS of each type within the first and second half of the acquisition phase (24 trials, respectively) and 6 CS of each type in the first and second half of the extinction phase (18 trials, respectively). During extinction training, CS order presentation was fully randomized.

The software Presentation (www.neurobs.com) was used to present visual stimuli, trigger application of thermal stimuli and record behavioural data.

Noxious thermal stimulation. Moderate continuous pain was elicited using a combined capsaicin and tonic heat model[14,15], which allows low-level heat stimuli to evoke moderate continuous heat pain that mimics clinical pain with lasting effects through controllable temperature manipulations[45]. Capsaicin cream (1%, 8-methyl-Nvanillyl-6-nonenamide, 98%, Sigma, diluted in 5% ethanol-KY jelly) was applied to the volar forearm over an area of 3 × 3 cm. After approximately 45 min, the capsaicin cream was removed and thermal stimulation (Model ATS, Pathway System, Medoc, Israel) was applied to the capsaicin pre-treated area, using a 3 × 3 cm probe. The individual heat pain threshold and temperature levels were then determined using a validated temperature calibration procedure[15] (see below and Supplementary Methods Temperature calibration).

Calibration procedure. An established/previously published adaptive multi-step calibration procedure was used to determine the individual temperatures resulting in the aspired pain percepts for the US in the experiment. The procedure involved the application of heat pain stimuli with varying intensities and durations and (subsequent) pain intensity ratings using a Visual Analogue Scale (VAS, 0–100, details see Behavioural outcome measures). A continuous/tonic medium intense pain perception was realized through continuous heat application (VAS40, US_{medium}). Phasic increases (VAS80, $US_{increase}$) and decreases (VAS0, $US_{decrease}$) in pain perception were realized through temporary changes in the applied temperature (temperature change: ramps 10 °C/s, plateau: duration 8 s) (for more detail see Supplementary Methods Temperature calibration). As in most experimental pain studies, individual pain thresholding and calibration represent an inherent limitation of pain psychophysics, as calibrated stimulus intensities may not remain perceptually equivalent over time. In the present study, individual calibration was performed both on the preparatory day in the laboratory and again on the experimental day inside the MRI scanner to ensure that the applied temperatures elicited the intended perceptual intensities. Pain intensity ratings were collected throughout the experiment to monitor perceptual responses over time. Importantly, ratings for the control condition (US_{medium}), in which stimulus intensity remained constant, did not show systematic changes over the course of the acquisition phase (see Supplementary Results US pain intensity and US (un)pleasantness).

Visual cues. Three geometric figures (a square, rectangle and rhombus; RBG: 142,180,227; visual angles: square 4.99° × 4.99°, rectangle 8.3° × 3.14°, rhombus 7.38° × 5.36°) served as CS ($CS_{increase}$, $CS_{decrease}$, CS_{medium}) to predict pain exacerbation ($US_{increase}$), pain decrease ($US_{decrease}$) and no change in temperature (US_{medium}), respectively.

Behavioural outcome measures

Behavioural measures were provided using VAS. Note that the numerical values of the anchors were never visible to the participants. Prior to habituation, participants rated their current arousal level ("How tense do you feel at the moment?", anchors: from "not tense at all" to "extremely tense") and pain-related fear ("How fearful are you about the upcoming pain stimulation?", anchors: from "not fearful at all" to "extremely fearful") using VAS 0–100.

To track the temporal dynamics of the acquisition and extinction of CS-US associations at the emotional and the cognitive level[5,15], participants provided ratings for CS valence ("How do you perceive this geometric figure?", anchors: −50 = "very pleasant", 0 = "neutral", and 50 = "very unpleasant") and CS-US contingency ("How often was this geometric figure followed by a painful stimulus?", anchors: −100 = "100% cold stimulus", 0 = "no change", 100 = "100% heat stimulus") using a VAS. The VAS were displayed for 7 s, beginning at the onset of the corresponding CS presentation. At the beginning of the habituation phase, participants provided one valence rating for each CS type. Further valence ratings were collected on every fourth CS presentation during acquisition training (four ratings per CS type) and extinction training (three ratings per CS type). CS-US contingency ratings were given at the end of both acquisition and extinction training, with no time limit imposed.

Ratings of US pain intensity and (un)pleasantness during acquisition and extinction training were collected using VAS (US pain intensity: "How painful was this temperature stimulus"; anchors: 0 = "not painful at all" and 100 = "unbearably painful"; US (un)pleasantness: "How pleasant/unpleasant was this temperature stimulus?"; anchors: −50 = "very pleasant", 0 = "neutral" and 50 = "very unpleasant"). US pain intensity and (un)pleasantness ratings were collected on every fourth US of the same type. Participants were given 15 s to rate each question, with an ITI of 0.5 s between questions. After confirming their responses for US pain intensity, the fixation cross of the ITI was immediately displayed, followed by the US (un)pleasantness rating (duration of US ratings: individual reaction time). This resulted in three ratings for each US type during acquisition training and five ratings for US_{medium} during extinction training. For each rating, the VAS cursor was placed at a random starting position between VAS25 and VAS75. Participants were instructed to confirm their responses, and the confirmed ratings were used for behavioural analyses. Except for contingency and US ratings, the VAS presentation remained on screen after confirmation until the next event started. Supplementary Table S6 provides a summary of the number of CS/US presentations and ratings.

Physiological outcome measures

Skin conductance data was recorded using a BIOPAC MP150 system with the software AcqKnowledge 4.2 (BIOPAC Systems Inc) at a sampling rate of 2 kHz. Two disposable Ag/AgCl electrodes (0.8 cm diameter) with conductive electrode cream (SYNAPSE ®; Kustomer Kinetics) were attached to the thenar and hypothenar eminences of the left hand for bipolar recording.

Due to technical issues, skin conductance data from $n = 41$ participants had to be excluded ($n = 15$ due to the original recordings measuring skin conductance responses (SCR) instead of skin conductance level recordings, thus not allowing the use of our preprocessing pipeline, $n = 14$ due to zero line recordings, $n = 8$ due to missing triggers, $n = 3$ due to noise, $n = 1$ due to electrode detachment), leaving a dataset of $n = 27$ for SCR

analyses (see Supplementary physiological analyses and Supplementary physiological results).

Data analysis

Consistent with our previous work using the same paradigm[15], our primary analyses of all learning-related outcome measures focused on differential contrasts (e.g., $CS_{increase}$ and $CS_{decrease}$ relative to CS_{medium}), as this approach allows a direct comparison of learning associated with pain increase and pain relief within the same tonic pain context. Importantly, the US_{medium} condition was not intended to represent a neutral baseline, but rather to approximate the ongoing tonic pain state. Please note that, in addition to the primary LMM analyses, we conducted complementary exploratory analyses to address specific aspects of acquisition and extinction that were not directly captured by the primary models. These analyses were prespecified as complementary analyses to provide additional information on the dynamics and extent of learning and extinction.

Behavioural analyses

Behavioural analyses of CS valence ratings, contingency ratings, US intensity and (un)pleasantness ratings were carried out in R version 4.1.1[46]. To compare aversive and appetitive acquisition and extinction learning, linear mixed models (LMM) were estimated using the lme4 package[47] (version 1.1-31) for each learning phase separately. In general, models were estimated using the restricted maximum likelihood (REML) approach and always included the factors specified in the model design as fixed effects (see below for the individual models and Supplementary Table S7). First, significant model improvement was tested by including a random intercept by participant. Second, improvement was tested by adding random slopes by CS (or US) type. All model comparisons were assessed using likelihood ratio tests and a reduction in the Akaike's information criterion (AIC). If the addition of a factor significantly improved the model fit, the more complex LMM was used. The significance of the included factors, as well as their interactions, were assessed using Type III Analysis of Variance Table with Satterthwaite's method. We report beta values from the model results when they are sufficient for interpretation (i.e., in the case of significant main effects involving only the respective factors). For specific differences in significant interaction effects, we report post-hoc tests carried out using the emmeans package[48] (version 1.8.3). A correction for multiple testing was applied using the Tukey or Sidak method where appropriate.

US intensity and US (un)pleasantness

Ratings of US pain intensity and US (un)pleasantness were analysed using LMMs to ensure that the calibration procedure was successful and that the three stimulation temperatures implemented as $US_{increase}$, US_{medium} and $US_{decrease}$ yielded different pain intensities and (un)pleasantness levels during the acquisition phase. For detailed results see Supplementary Results US pain intensity and US (un)pleasantness.

CS valence

To assess acquisition and extinction learning on the behavioural level, CS valence ratings were analysed using a LMM with participant as a random effect (random intercepts, and random slopes by *CS type*), and *CS type* and *time* (continuous), as well as their interaction, as fixed effects. CS valence ratings were first analysed differentially, i.e., relative to the CS_{medium} (i.e., $CS_{increase} - CS_{medium}$; $CS_{medium} - CS_{decrease}$), to directly compare the level of CS-US associations between the increase and decrease conditions. In a second model, ratings for each of the three conditions were entered. Models were estimated separately for each phase, including the final rating from the previous phase as the baseline (i.e., the factor time comprised ratings H0 – A4 for acquisition training and A4 – E3 for extinction training, resulting in 5 and 4 ratings per CS type within the phases, respectively; see Fig. 2). Models included fixed effects of *CS type* ($CS_{increase}$, CS_{medium}, and $CS_{decrease}$, or $CS_{increase}$ and $CS_{decrease}$ (relative to the CS_{medium})) as a categorical factor and *time* as a continuous variable, as well as their interaction. Additionally, we conducted an exploratory comparison of the aversive and appetitive conditions using two-sided paired *t*-tests on individual slopes. To investigate whether the valence ratings obtained at the end of the conditioning task (i.e., after extinction training) had returned to baseline (i.e., habituation phase), which would suggest the complete extinction of the acquired CS-US associations, we performed exploratory post-hoc comparisons using the first and last valence ratings for the $CS_{increase}$ and $CS_{decrease}$.

CS-US contingency

To investigate acquisition and extinction learning on the cognitive level, we analysed CS-US contingency ratings provided at the end of each learning phase. CS-US contingency ratings were transformed so that positive values represented correct learning (i.e., $CS_{decrease}$ value x (−1)). Models included the same fixed effects factors as described for CS valence, including all three levels of *CS types* (i.e., $CS_{increase}$, CS_{medium}, $CS_{decrease}$), except that *timepoint* was added as a categorical factor (i.e., rating after acquisition, and after extinction training only). To test for incomplete extinction for the aversive or appetitive condition, CS-US contingency ratings were compared against 0 by phase and CS type using post-hoc comparisons.

fMRI data acquisition and analysis

MRI data acquisition and preprocessing. MRI data were collected on a 3.0 Tesla scanner (Siemens Trio) with a 32-channel head coil. Functional images were obtained using a gradient EPI T2*-weighted sequence for each participant with the following acquisition parameters: repetition time (TR), 2.19 s; echo time (TE), 26 ms; slices number, 42; slice-thickness, 2.5 mm; field of view (FOV), 224 × 224 mm; voxel size, 2.5 × 2.5 × 2.5 mm; flip angle, 90°. High-resolution whole-brain T1-weighted images were acquired using an MP-RAGE sequence with TR, 1.77 s; TE, 3.24 ms; slices number, 224; slice-thickness, 1 mm; FOV, 256 × 256 mm; flip angle, 8°.

Neuroimaging data were preprocessed using the fMRIprep v22.1.1 pipeline[49]. Preprocessing of participants' T1-weighted images included skull-stripping, spatial normalization and brain tissue segmentation. Functional images were preprocessed separately for acquisition and extinction training, including co-registration with individual T1-weighted reference image, motion correction, slice-timing correction and normalization to MNI152NLin2009cAsym standard space. In each phase, physiological regressors were calculated using component-based noise correction (CompCor)[50], and the first 6 anatomical components (aCompCor) for each participant were added as nuisance regressors to the individual design matrix in the first-level analysis. Functional images were spatially smoothed using a Gaussian kernel with 6 mm full-width at half-maximum (FWHM).

fMRI data analysis. Univariate general linear model (GLM) analyses were conducted separately for the acquisition and extinction phases using SPM12 (https://www.fil.ion.ucl.ac.uk/spm/). The GLM structure was designed to capture distinct processes during the task. CS regressors modelled cue-evoked anticipatory processes, whereas US regressors modelled neural responses to noxious stimulation. Time modulation of the CS regressors captured systematic changes in cue responses during acquisition and extinction across trials reflecting learning. Note that because our primary interest was in learning-related changes in cue processing, the main analyses focused on CS-evoked activity and its modulation over time during acquisition and extinction. Analyses of neural responses to the US (pain increase and pain decrease) were conducted for completeness but are reported in the Supplementary Results Average neural activity underlying US events. Note that trials in which participants provided valence ratings were excluded from all CS-related BOLD analyses to avoid potential confounds arising from motor responses and any systematic differences in visual behaviour during rating.

To perform all planned analyses, individual design matrices (subject level) included 15 regressors. Six regressors of interest coded for the CS events ($CS_{increase}$, $CS_{decrease}$, CS_{medium}). Each CS event was modelled with

two regressors capturing an early response (starting at CS onset) and a late response (starting 4.5 s after CS onset) (modelled duration: 0 s), following an approach previously described[19]. This served two purposes. First, it captured temporally distinct cognitive processes rather than collapsing across the full CS presentation into a single estimate. Second, it enabled targeted investigation of the late anticipatory phase, motivated by evidence that neural responses to predicted pain peak immediately prior to US onset, a time-window in which anticipatory activity may remain elevated (i.e., show less decrease over time) in the case of incomplete extinction study[15]. For the main analyses investigating cue-related learning effects, early and late CS responses were combined to capture overall cue-evoked activity. To evaluate potential multicollinearity, we computed the cosine of the angle between regressor pairs and variance inflation factors, which revealed consistently low values, confirming negligible collinearity[51,52] (Supplementary Results Design matrix orthogonality tests & Fig. S3). To assess whether our primary findings depended on the two-regressor modelling strategy, we additionally conducted a GLM analysis in which each CS type was modelled with a single boxcar regressor spanning the full CS duration, which revealed replicated acquisition effects and minor divergence during extinction (Supplementary Results Sensitivity analysis using the GLM with single CS regressors).

To examine brain activity during noxious stimulation in the acquisition phase (pain exacerbation and pain relief), two regressors modelling $US_{increase}$ and $US_{decrease}$ (duration: 8 s) were added to the individual design matrices. For both phases, the individual design matrices also included 7 nuisance variables controlling for motion-related artefacts, including head movement (6 aCompCor components) and ratings (valence: duration 7 s; US pain intensity and (un)pleasantness: duration individual rating time, maximum 15 s per question). CS, US and nuisance regressor corresponding to rating periods were each convolved with the canonical hemodynamic response function. To model learning-related dynamics over the course of each phase, CS regressors were parametrically modulated by time (trial order), capturing linear changes in cue-evoked activity during acquisition and extinction as described previously[39].

Individual-level contrasts images for time-modulated CS events (combining early and late CS responses: [$CS_{increase\ x\ time} - CS_{medium\ x\ time}$], [$CS_{decrease\ x\ time} - CS_{medium\ x\ time}$]) and contrast images modelling individual US conditions (acquisition training: $US_{increase}$, $US_{decrease}$) were entered into group-level analyses.

The following four types of analyses were performed to answer our research questions:

(1) Common neural responses during aversive and appetitive learning. To identify brain regions showing learning-related activity common to both aversive and appetitive conditioning, we performed conjunction analyses of the contrast ([$CS_{increase\ x\ time} - CS_{medium\ x\ time}$] ∩ [$CS_{decrease\ x\ time} - CS_{medium\ x\ time}$]), conducted separately for the acquisition and the extinction phase[53].

(2) Distinct neural responses during appetitive and aversive learning. To identify differences between aversive and appetitive learning during acquisition and extinction learning, differential contrasts ([$CS_{increase\ x\ time} - CS_{medium\ x\ time}$] > [$CS_{decrease\ x\ time} - CS_{medium\ x\ time}$] and [$CS_{increase\ x\ time} - CS_{medium\ x\ time}$] < [$CS_{decrease\ x\ time} - CS_{medium\ x\ time}$] were calculated for CS events and entered into group-level one-sample *t*-tests. Note that consistent with our learning framework, the primary analysis focuses on systematic changes in CS-evoked activity over time during acquisition and extinction, reflecting learning-related neural dynamics rather than static condition differences.

Neural responses to aversive and appetitive learning over the course of acquisition and extinction training were analysed (e.g., $CS_{increase\ x\ time} > CS_{medium\ x\ time}$) and are shown in Supplementary Tables S8 and S9.

(3) Time-modulated functional connectivity during learning. To further examine how the regions identified in the activation analyses (see analyses 1 and 2) interact with other brain regions during learning, we conducted psychophysiological interaction analyses using gPPI[54] to characterize their functional connectivity, separately for the acquisition phase and the extinction phase. Seed regions were defined based on clusters identified in the activation analyses. For each seed region, first-level gPPI models included (i) psychological regressors corresponding to the task condition (identical to those in the activation analysis; e.g., $CS_{increase\ x\ time}$), (ii) physiological regressor representing the time series extracted from the seed region and (iii) psychophysiological interaction terms reflecting the interaction between the seed region time series and each task condition. To examine how connectivity evolved during learning, the interaction terms were parametrically modulated by time (trial order), which allows us to test whether functional coupling between the seed region and other regions changed over the course of acquisition or extinction, respectively. For instance, a significantly positive result reveals an increase over time in functional coupling. For the seed regions showing shared activation changes over time in both conditions, connectivity was examined separately for appetitive and aversive learning using the corresponding contrasts ([$CS_{decrease\ x\ time} - CS_{medium\ x\ time}$], [$CS_{increase\ x\ time} - CS_{medium\ x\ time}$]). Differential connectivity between conditions was assessed using the contrast ([$CS_{increase\ x\ time} - CS_{medium\ x\ time}$] > [$CS_{decrease\ x\ time} - CS_{medium\ x\ time}$]) and ([$CS_{increase\ x\ time} - CS_{medium\ x\ time}$] < [$CS_{decrease\ x\ time} - CS_{medium\ x\ time}$]). Individual-level contrast images were then entered into group-level one-sample *t*-tests.

(4) Neural correlates of incomplete extinction. To explore neural processes underlying the incomplete extinction observed on the behavioural level (i.e., elevated contingency ratings for $CS_{increase}$ after extinction training; see Results), we took a two-step approach focusing on anticipatory activity during the late CS phase. In the first step, we identified brain regions exhibiting learning-related increases in activity during the late CS phase of acquisition using the contrast [$CS_{increase\ x\ time} - CS_{medium\ x\ time}$]. This analysis revealed a cluster in the occipital cortex as the only region surviving whole-brain correction. This cluster was then used as an ROI to examine extinction-related changes in anticipatory activity ($p_{SVC\text{-}FWE} < 0.05$). In the second step, we tested whether extinction-related signal changes in this occipital ROI were associated with behavioural evidence of incomplete extinction. Specifically, activation change in this cluster during extinction was correlated with the behavioural index of incomplete extinction (i.e., contingency rating of $CS_{increase} - CS_{medium}$ after extinction) by Pearson correlation. BOLD signal estimates were extracted from the activated cluster using MarsBaR[55].

We used a region-of-interest approach on brain networks involved in pain, learning, reward processing and salience[7,9,56–59]. ROIs included the orbitofrontal cortex, vmPFC, dorsomedial prefrontal cortex, frontal operculum, insula, primary somatosensory cortex, secondary somatosensory cortex, thalamus, PHG, hippocampus, amygdala, striatum, ventral tegmental area, and brainstem. The brainstem ROI (i.e., locus coeruleus) was defined using the probabilistic anatomical grey matter masks[60,61]. The masks were thresholded at $p > 70\%$ grey matter probability, resulting in a binary mask (https://osf.io/xqvb6) applied directly for small-volume correction (SVC). All other ROIs were defined using anatomical masks based on Harvard-Oxford cortical and subcortical 25% probability atlases[62]. Within these regions, SVC analyses were conducted. Statistical maps were thresholded at a voxel-level (cluster-forming) threshold of $p_{uncorrected} < 0.001$, with significance defined at peak-level family-wise error (FWE) rate of $p_{SVC\text{-}FWE} < 0.05$ separately for each ROI. For whole-brain analyses, the same voxel-level threshold ($p_{uncorrected} < 0.001$) was applied, and clusters were considered significant at a cluster-level $p_{cluster\text{-}FWE} < 0.05$[63]. Subregion identification for the occipital cortex was based on Julich-Brain Cytoarchitectonic Atlas[64] and The Thalamus Atlas[65] for the thalamus. Additional supplementary analyses examining condition-specific responses were conducted using a liberal uncorrected threshold

($p < 0.001$) and should be considered exploratory (results see Supplementary imaging results).

Statistics and reproducibility

Analyses of behavioural data were carried out in R version 4.1.1[46]. LMM were used to assess learning in each phase separately, followed by two-tailed post-hoc tests with adjustments for multiple testing using the Tukey or Sidak method. Additionally, two-sided paired *t*-tests were used to compare individual valence slopes, and a linear model to compare early valence learning during acquisition training. Tests were considered statistically significant at a level of $p < 0.05$. Data are presented as means ± confidence intervals, sample sizes are indicated in the figure legends.

For neuroimaging data, first-level GLMs were estimated in SPM12 v7771 (MATLAB R2024a), followed by group-level analyses of brain activation and functional connectivity[54] using one-sided *t*-tests for directional contrasts ($n = 61$). Pearson correlation between the behavioural measure and brain activity change (i.e., neural correlates of incomplete extinction) were conducted in Python 3.10.9 (scipy.stats.pearsonr; two-sided). Main analysis code is available as stated in Code availability.

Data availability

Behavioural, physiological, and neuroimaging data for figure reproduction are available at https://figshare.com/s/a23998efe1672eb711e0[66]. Neuroimaging results shown in the Manuscript and Supplementary Information are accessible via NeuroVault at https://neurovault.org/collections/MXFFKNVE.

Code availability

The code for reproducing the main figures is available at https://figshare.com/s/a23998efe1672eb711e0[66]. For behavioural (Fig. 2 and Supplementary Fig. S1) and physiological (Supplementary Fig. S2) code, R version 4.1.1 was used, with the following package versions: here 1.0.2, ggplot2 4.0.3, ggpubr 0.5.0, and ggdist 3.2.0. Figures 3–5 and Supplementary Fig. S3 were produced in Python 3.10.9 using NumPy 1.26.4, pandas 2.2.3, SciPy 1.15.0, Matplotlib 3.7.0 and seaborn 0.13.2, with neuroimaging visualization performed in Mango 4.1 (http://ric.uthscsa.edu/mango/) and MRIcroGL 1.2.20210930 (https://www.nitrc.org/projects/mricrogl/).

Received: 30 April 2026; Accepted: 21 October 2026;
Published online:

References

1. Wiech, K. & Tracey, I. Pain, decisions, and actions: a motivational perspective. *Front. Neurosci*. **7**, 46 (2013).
2. Chen, Z. S. & Wang, J. Pain, from perception to action: a computational perspective. *iScience* **26**, 105707 (2023).
3. Navratilova, E., Atcherley, C. W. & Porreca, F. Brain circuits encoding reward from pain relief. *Trends Neurosci.* **38**, 741–750 (2015).
4. Timmers, I. et al. Neural evidence for the effects of behavioral memory updating following fear conditioning. *Commun. Psychol.* **3**, 153 (2025).
5. Schlitt, F. et al. Impaired pain-related threat and safety learning in patients with chronic back pain. *Pain* **163**, 1560–1570 (2022).
6. Lanters, L. R. et al. Disease-specific alterations in central fear network engagement during acquisition and extinction of conditioned interoceptive fear in inflammatory bowel disease. *Mol. Psychiatry* **29**, 3527–3536 (2024).
7. Fullana, M. A. et al. Neural signatures of human fear conditioning: an updated and extended meta-analysis of fMRI studies. *Mol. Psychiatry* **21**, 500–508 (2016).
8. Corlett, P. R., Mollick, J. A. & Kober, H. Meta-analysis of human prediction error for incentives, perception, cognition, and action. *Neuropsychopharmacology* **47**, 1339–1349 (2022).
9. Klein, S. et al. Cross-paradigm integration shows a common neural basis for aversive and appetitive conditioning. *NeuroImage* **263**, 119594 (2022).
10. Gu, Y. et al. Neural activities underlying the feedback express salience prediction errors for appetitive and aversive stimuli. *Sci. Rep.* **6**, 34032 (2016).
11. Metereau, E. & Dreher, J.-C. The medial orbitofrontal cortex encodes a general unsigned value signal during anticipation of both appetitive and aversive events. *Cortex* **63**, 42–54 (2015).
12. Kim, J.-C., Hellrung, L., Nebe, S. & Tobler, P. N. The anterior insula processes a time-resolved subjective risk prediction error. *J. Neurosci*. **45**, e2302242025 (2025).
13. Petrenko, M. et al. Appetitive and aversive classical conditioning: Self-reports and physiological responses. *Behav. Brain Res.* **484**, 115509 (2025).
14. Seymour, B. et al. Opponent appetitive-aversive neural processes underlie predictive learning of pain relief. *Nat. Neurosci.* **8**, 1234–1240 (2005).
15. van der Schaaf, M. E. et al. Acquisition learning is stronger for aversive than appetitive events. *Commun. Biol.* **5**, 1–10 (2022).
16. Andreatta, M. & Pauli, P. Appetitive vs. Aversive conditioning in humans. *Front. Behav. Neurosci*. **9**, 128 (2015).
17. Colloca, L., Sigaudo, M. & Benedetti, F. The role of learning in nocebo and placebo effects. *Pain* **136**, 211–218 (2008).
18. Kunkel, A. et al. Nocebo effects are stronger and more persistent than placebo effects in healthy individuals. *eLife* **14**, RP105753 (2025).
19. Eippert, F., Bingel, U., Schoell, E., Yacubian, J. & Buchel, C. Blockade of endogenous opioid neurotransmission enhances acquisition of conditioned fear in humans. *J. Neurosci.* **28**, 5465–5472 (2008).
20. Battistoni, E., Stein, T. & Peelen, M. V. Preparatory attention in visual cortex. *Ann. N. Y. Acad. Sci.* **1396**, 92–107 (2017).
21. Li, W. & Keil, A. Sensing fear: fast and precise threat evaluation in human sensory cortex. *Trends Cogn. Sci.* **27**, 341–352 (2023).
22. Sehlmeyer, C. et al. Human fear conditioning and extinction in neuroimaging: a systematic review. *PLoS ONE* **4**, e5865 (2009).
23. Neumann, N. et al. Common neural correlates of vestibular stimulation and fear learning: an fMRI meta-analysis. *J. Neurol.* **270**, 1843–1856 (2023).
24. Wolff, M. & Halassa, M. M. The mediodorsal thalamus in executive control. *Neuron* **112**, 893–908 (2024).
25. Zhang, X., Mukherjee, A., Halassa, M. M. & Chen, Z. S. Mediodorsal thalamus regulates task uncertainty to enable cognitive flexibility. *Nat. Commun.* **16**, 2640 (2025).
26. Sara, S. J. & Bouret, S. Orienting and reorienting: the locus coeruleus mediates cognition through arousal. *Neuron* **76**, 130–141 (2012).
27. Llorca-Torralba, M., Borges, G., Neto, F., Mico, J. A. & Berrocoso, E. Noradrenergic Locus Coeruleus pathways in pain modulation. *Neuroscience* **338**, 93–113 (2016).
28. Velayos, J. L. & Reinoso-Suarez, F. Topographic organization of the brainstem afferents to the mediodorsal thalamic nucleus. *J. Comp. Neurol.* **206**, 17–27 (1982).
29. Gottfried, J. A., O'Doherty, J. & Dolan, R. J. Appetitive and aversive olfactory learning in humans studied using event-related functional magnetic resonance imaging. *J. Neurosci.* **22**, 10829–10837 (2002).
30. Plassmann, H., O'Doherty, J. P. & Rangel, A. Appetitive and aversive goal values are encoded in the medial orbitofrontal cortex at the time of decision making. *J. Neurosci.* **30**, 10799–10808 (2010).
31. Bulganin, L., Bach, D. R. & Wittmann, B. C. Prior fear conditioning and reward learning interact in fear and reward networks. *Front. Behav. Neurosci*. **8**, 67 (2014).
32. McCabe, C. & Rocha-Rego, V. Investigating the predictive value of functional MRI to appetitive and aversive stimuli: a pattern classification approach. *PLoS ONE* **11**, e0165295 (2016).
33. Battaglia, S., Harrison, B. J. & Fullana, M. A. Does the human ventromedial prefrontal cortex support fear learning, fear extinction or both? A commentary on subregional contributions. *Mol. Psychiatry* **27**, 784–786 (2022).

34. Quirk, G. J., Garcia, R. & González-Lima, F. Prefrontal mechanisms in extinction of conditioned fear. *Biol. Psychiatry* **60**, 337–343 (2006).
35. Dunsmoor, J. E. et al. Role of human ventromedial prefrontal cortex in learning and recall of enhanced extinction. *J. Neurosci.* **39**, 3264–3276 (2019).
36. Milad, M. R. et al. Recall of fear extinction in humans activates the ventromedial prefrontal cortex and hippocampus in concert. *Biol. Psychiatry* **62**, 446–454 (2007).
37. Morriss, J., Hoare, S. & van Reekum, C. M. It's time: a commentary on fear extinction in the human brain using fMRI. *Neurosci. Biobehav. Rev.* **94**, 321–322 (2018).
38. Molapour, T., Golkar, A., Navarrete, C. D., Haaker, J. & Olsson, A. Neural correlates of biased social fear learning and interaction in an intergroup context. *NeuroImage* **121**, 171–183 (2015).
39. Forkmann, K., Wiech, K., Schmidt, K., Schmid-Köhler, J. & Bingel, U. Neural underpinnings of preferential pain learning and the modulatory role of fear. *Cereb. Cortex* **33**, 9664–9676 (2023).
40. Pacheco-Estefan, D. et al. Representational dynamics during extinction of fear memories in the human brain. *Nat. Hum. Behav.* **10**, 29–48 (2026).
41. Bouton, M. E. Context and behavioral processes in extinction. *Learn. Mem.* **11**, 485–494 (2004).
42. Schiller, D. & Delgado, M. R. Overlapping neural systems mediating extinction, reversal and regulation of fear. *Trends Cogn. Sci.* **14**, 268–276 (2010).
43. Lonsdorf, T. B. et al. Don't fear 'fear conditioning': methodological considerations for the design and analysis of studies on human fear acquisition, extinction, and return of fear. *Neurosci. Biobehav. Rev.* **77**, 247–285 (2017).
44. Forkmann, K. et al. Pain-specific modulation of hippocampal activity and functional connectivity during visual encoding. *J. Neurosci.* **33**, 2571–2581 (2013).
45. Petersen, K. L. & Rowbotham, M. C. A new human experimental pain model: the heat/capsaicin sensitization model. *NeuroReport* **10**, 1511 (1999).
46. R Core Team. R: A language and environment for statistical computing (2021).
47. Bates, D., Mächler, M., Bolker, B. & Walker, S. Fitting linear mixed-effects models using lme4. *J. Stat. Soft*. **67**, 1–48 (2015).
48. Lenth, R. V. emmeans: Estimated marginal means, aka least-squares means. R package version 1.8.3. (2022).
49. Esteban, O. et al. fMRIPrep: a robust preprocessing pipeline for functional MRI. *Nat. Methods* **16**, 111–116 (2019).
50. Behzadi, Y., Restom, K., Liau, J. & Liu, T. T. A component based noise correction method (CompCor) for BOLD and perfusion based fMRI. *NeuroImage* **37**, 90–101 (2007).
51. Mumford, J. A., Poline, J.-B. & Poldrack, R. A. Orthogonalization of regressors in fMRI models. *PLoS ONE* **10**, e0126255 (2015).
52. Kim, J. H. Multicollinearity and misleading statistical results. *Korean J. Anesthesiol.* **72**, 558–569 (2019).
53. Nichols, T., Brett, M., Andersson, J., Wager, T. & Poline, J.-B. Valid conjunction inference with the minimum statistic. *NeuroImage* **25**, 653–660 (2005).
54. McLaren, D. G., Ries, M. L., Xu, G. & Johnson, S. C. A generalized form of context-dependent psychophysiological interactions (gPPI): a comparison to standard approaches. *NeuroImage* **61**, 1277–1286 (2012).
55. Brett, M., Anton, J.-L., Valabregue, R. & Poline, J.-B. Region of interest analysis using an SPM toolbox. *NeuroImage* **16**, https://doi.org/10.1016/S1053-8119(02)90013-3 (2002).
56. Briggs, R. G. et al. Parcellation-based tractographic modeling of the salience network through meta-analysis. *Brain Behav.* **12**, e2646 (2022).
57. Hayes, D. J., Duncan, N. W., Xu, J. & Northoff, G. A comparison of neural responses to appetitive and aversive stimuli in humans and other mammals. *Neurosci. Biobehav. Rev.* **45**, 350–368 (2014).
58. Wager, T. D. et al. An fMRI-based neurologic signature of physical pain. *N. Engl. J. Med.* **368**, 1388–1397 (2013).
59. Radua, J. et al. Neural correlates of human fear conditioning and sources of variability in 2199 individuals. *Nat. Commun.* **16**, 7869 (2025).
60. Oliva, V., Hartley-Davies, R., Moran, R., Pickering, A. E. & Brooks, J. C. Simultaneous brain, brainstem, and spinal cord pharmacological-fMRI reveals involvement of an endogenous opioid network in attentional analgesia. *eLife* **11**, e71877 (2022).
61. Brooks, J. C. W., Davies, W.-E. & Pickering, A. E. Resolving the brainstem contributions to attentional analgesia. *J. Neurosci.* **37**, 2279–2291 (2017).
62. Desikan, R. S. et al. An automated labeling system for subdividing the human cerebral cortex on MRI scans into gyral based regions of interest. *NeuroImage* **31**, 968–980 (2006).
63. Woo, C.-W., Krishnan, A. & Wager, T. D. Cluster-extent based thresholding in fMRI analyses: Pitfalls and recommendations. *NeuroImage* **91**, 412–419 (2014).
64. Amunts, K., Mohlberg, H., Bludau, S. & Zilles, K. Julich-Brain: a 3D probabilistic atlas of the human brain's cytoarchitecture. *Science* **369**, 988–992 (2020).
65. Krauth, A. et al. A mean three-dimensional atlas of the human thalamus: generation from multiple histological data. *NeuroImage* **49**, 2053–2062 (2010).
66. Li, J. et al. Data and code for "Shared and distinct neural pathways of aversive and appetitive pain-related learning". https://doi.org/10.6084/m9.figshare.c.8751054 (2026).

Acknowledgements

We would like to thank Matthias Gamer and Balint Kincses for conceptual and methodological support.

Author contributions

Conceptualization: K.S., K.F., and U.B. Methodology: J.L., K.S., L.B., T.S., K.F., K.W., and U.B. Investigation: J.K. and F.S. Supervision: K.S. and U.B. Writing—original draft: J.L., K.S., L.B., K.W., K.F., and U.B. Writing—review & editing: J.L., K.S., L.B., K.W., K.F., and U.B.

Funding

German Research Foundation – project A11, project number 316803389 – SFB 1280 (Gefördert durch die Deutsche Forschungsgemeinschaft (DFG) – Projekt A11, Projektnummer 316803389 – SFB 1280). Open Access funding enabled and organized by Projekt DEAL.

Competing interests

The authors declare no competing interests.

Additional information

Supplementary information The online version contains supplementary material available at https://doi.org/10.1038/s42003-026-11323-4.

Correspondence and requests for materials should be addressed to Katharina Schmidt.

Peer review information *Communications Biology* thanks all reviewer(s) for their contribution to the peer review of this work. Primary handling editors: Lei Zhang and Jasmine Pan.

Reprints and permissions information is available at http://www.nature.com/reprints

Publisher's note Springer Nature remains neutral with regard to jurisdictional claims in published maps and institutional affiliations.

Open Access This article is licensed under a Creative Commons Attribution 4.0 International License, which permits use, sharing, adaptation, distribution and reproduction in any medium or format, as long as you give appropriate credit to the original author(s) and the source, provide a link to the Creative Commons licence, and indicate if changes were made. The images or other third party material in this article are included in the article's Creative Commons licence, unless indicated otherwise in a credit line to the material. If material is not included in the article's Creative Commons licence and your intended use is not permitted by statutory regulation or exceeds the permitted use, you will need to obtain permission directly from the copyright holder. To view a copy of this licence, visit http://creativecommons.org/licenses/by/4.0/.

© The Author(s) 2026